Investigation of pressure swirl sprays using Volumetric PIV

Ondřej Cejpek*[1], Milan Malý[1], Amine Koched[2], Marcel Sapík[1], František Lízal[1], Jan Jedelský[1]
[1]Energy Institute, Faculty of Mechanical Engineering, Brno University of Technology,
Technická 2896/2, 616 69 Brno, Czech Republic
[2]TSI France Inc., Hotel Technologique BP100, Technopole de Château Gombert, 13382
Marseille Cedex 13, France
*Corresponding author: 182752@vutbr.cz

Abstract

The volumetric measurement technique (V3V-Flex©) was used to investigate the spray generated by two pressure swirl atomizers (PSAs). Both a simplex pressure swirl atomizer and a spill-return pressure swirl atomizer were investigated. In this paper the experimental setup is briefly described and the essential functions and differences between the atomizers are outlined. The fundamental principles of the volumetric measurement technique are described. The behaviour of the PSAs under different test conditions is presented, and a comparison of the droplet flow field is made.

Keywords

V3V-Flex©, pressure swirl atomizer, flow field, volumetric PIV

Introduction

PSAs are widely used in gas turbine combustors, industrial and domestic burners, rocket engines and agriculture. PSAs use the pressure energy of the pumped liquid to atomize the bulk liquid; the pressure energy is converted into kinetic energy; this process creates a high-speed swirling liquid cone. The atomization process consists of the discharge of the liquid through the orifice, the formation of a liquid film and then downstream its breakup into droplets and the interaction of the droplets with a surrounding air. Phenomena such as droplet clustering, droplet collisions, droplet streaking and interaction of droplets with the surrounding medium have been observed [1].

So far, point wise (LDA/PDA) and planar (2D2C or 2D3C PIV) [2] are common methods or high-speed imagining have used as non–intrusive diagnostic methods to investigate the spray flow in terms of droplet velocity, droplet/particle diameter, a spray cone angle, etc. As the volumetric methods are a recent development, they can provide new insight into the spray flow characteristics and advance our understanding of these complex two-phase flows.

The 3D3C V3V-Flex© measurement system (TSI Inc., 2016) was used for this investigation of the velocity field in a spray generated by two types of pressure swirl atomizers (PSA); "spill-return" and "simplex" versions. The former atomizer was investigated under three operating regimes while the later under two operating conditions defined by the inlet over-pressure and the flow rate at the atomizer exit. The sprays produced by these PSAs represents a very complex 3D flow structure, with a swirling motion of the liquid film close to the nozzle and the radial development of the droplets downstream. The droplet concentration is very high and spatially variable, and the spray produces a wide range of droplet sizes, ranging from micron to more than 100 µm. The size of the measurement volume covered approximately two thirds of the spray volume. The measurement volume size was limited by the small diameter of the spray droplets used as natural seeding and by the energy of the light laser source.

Experimental setup

The PSAs were investigated with the V3V-Flex© system at TSI GmbH fluid Mechanics Laboratory in Aachen, Germany. [3]. Figure 1 shows the experimental setup. V3V-Flex© is a volumetric PIV technique based on previous "triangle shaped" version of the V3V-9000. Higher temporal and spatial resolution, better flexibility could be achieved with V3V-Flex© system.

The PSAs were located in a nozzle housing, which was connected to the reservoir water system. These two line from atomizer was directed into a collecting vessel. Control valves and pressure gauges, with measuring range of 16 bar and accuracy of 0.256 bar, monitored the inlet and outlet flows. The maximum considered pressure was 4.5 bar.

Water was used as a working fluid with no additional particles. The water droplets created during atomization were used as flow tracers. These PSAs are normally used with Jet-A1 fuel as the working fluid. Water has slightly different properties to the Jet-A1 fuel (kerosene). Effect of the different densities between water and kerosene (30 %) on atomization quality is almost negligible [4]. However, the surface tension of the water is almost three times larger than that of the kerosene and this difference does affect the SMD and atomization quality significantly. The properties of water and Jet-A1 fuel are presented in Table 1.

Table 1. Properties of water and kerosene

	Water	*Jet-A1*
Surface tension $[kg/s^2]$	0.072	0.029
Dynamic viscosity $[kg/m \cdot s]$	0.00089	0.0016
Density $[kg/m^3]$	997	795
Refractive index [–]	1.33	1.44

The operating conditions for the PSAs are reported in Table 2.

Table 2. Test conditions

	Spill-return PSA	*Simplex PSA*
1	P_{in} = 4.5 bar, SL = closed	P_{in} = 4.5 bar
2	P_{in} = 4.5 bar, SL = open	P_{in} = 3.5 bar
3	P_{in} = 3.5 bar, SL = closed	–

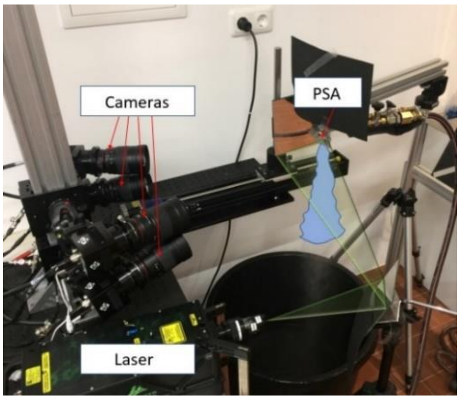

Figure 1. Experimental setup

Pressure swirl atomizer

Pressure swirl atomizers are composed of three or more tangential inlet ports, through which, the working fluid is supplied into the swirl chamber. The swirling working fluid is then discharged into the surrounding environment via the discharge orifice. The design of the PSAs is almost the same, except that the spill-return pressure swirl atomizer contains a (bypass) spill-line (SL) at the rear back of the swirl chamber. A portion of the fluid flows through spill-line and does not undergo atomization process. Schematic layout of the PSAs are shown in Figure 2. A simplex pressure swirl atomizer has a limited flow rates and regulation range [4], while the spill-line in Spill-return pressure swirl atomizer overcomes this problem. [5]

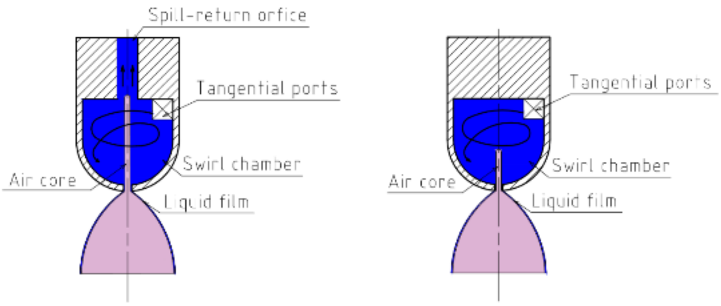

Figure 2. Pressure swirl atomizers

PSAs create a hollow cone spray; most of the fluid volume of this spray is concentrated on the spray periphery. One of the main spray characteristics is the spray cone angle. These varies mainly according to changes mainly with inlet pressure and SL adjustment and only slightly with the changes in fluid properties.
In the spray, there are two breakup regions. The primary breakup region is where liquid sheet forms into ligaments and the secondary breakup region is where the ligaments disintegrate into droplets i.e atomization. This is a very fast but chaotic process in which a wide range of droplet diameters is created, ranging from microns to more than 100 microns.

V3V-Flex© system

The V3V-Flex© is a volumetric measurement technique. Its function is based on volumetric particle tracking velocimetry (PTV). For each individual particle captured in an image of measurement volume, PTV can construct the particle velocity vector. The advantage of PTV lies in less ghost particles being created during the computational process as found by other methods such as tomographic PIV or holographic PIV [6]. It also offers a higher accuracy during fluid flow measurements, where high-velocity gradients are present. The number of a velocity vectors created depends on the number of seeding particles in the measurement volume.

Calibration

In order to make an accurate volume flow measurement, it is crucial to perform a calibration of the measurement volume. The purpose of the calibration is to map the captured image coordinates, x–y, to real-world coordinates (X,Y,Z). The V3V-Flex© system automatically corrects camera imperfections such as mechanical misalignments of CCD sensors and optical aberrations of the lenses. At least three cameras must be used to accurately reconstruct the position of the particles/droplets in the 3D volume of measurement. In these experiment 4 cameras were used. A calibration target of 200×200 mm with uniformly spaced dots, in the X–Y direction, of 5×5 mm was used. During the calibration process the calibration target was traversed in the Z direction, through the measurement volume, with equidistant steps of 2 mm. There are three missing dots in the calibration target centre used as a mark for grid origin.

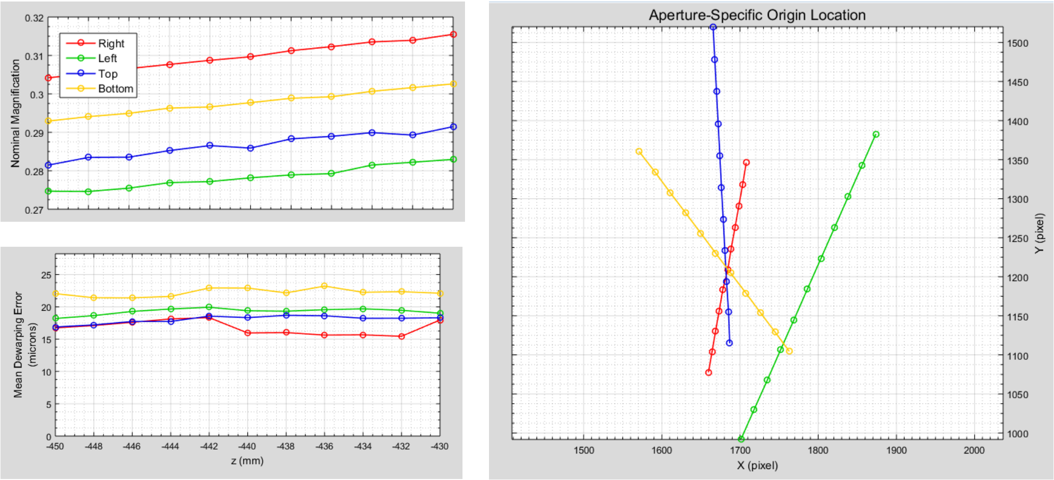

Figure 3. Calibration results

Mean dewarping error approximately 20 µm is shown on the LHS Fig.3 as a function of Z. It also contains a magnification function for each camera used in the experiment. The aperture-specific Origin Location marks the position of the grid origin of the calibration plate across the volume of measurement for each camera.

Image processing

A set of 4 raw images captured by the software are shown below in Fig. 4. The images show that there are some saturated pixels (i.e. pink pixels). To improve the contrast between the particle images and the background a pre-processing is applied to each instantaneous capture. This consists of subtracting from each pixel count the local mean intensity calculated from the surrounding 7×7 pixels. Each droplet is represented by a spot of light of only a few pixels captured by the camera on the raw images. This corresponds to the Mie scattering of laser light by the droplet which might not be isotropic so, as part of the pre-processing, a Gaussian filter is applied to the raw images to improve the shape of the pixelated droplets. The next step after this pre-processing consists in identifying the individual particles via a Levenberg-Marquardt non-linear solver that takes into account a defined threshold value, min and max radius values in pixels, as defined by the user, and a percentage of overlap of 50 % that may occur between the droplets. Typically, at this step around 30´000 droplets are identified for each capture. The next step in the processing consists of matching the identified particles between the cameras to find the common particle.

The mapping function M (calculated from the calibration) is used at this step to map each particle image from the right camera into physical coordinates which will be mapped back into every other camera, using M^{-1} (x,y) to define the search area. This area constitutes a set of all possible locations of a given particle image, within an aperture. All particle images in the search area are mapped into physical space. Those particle images which intersect, within the user-prescribed tolerance, in microns, are considered as a particle match. The process is done for all calibration planes, and all particle images from the left camera are processed. Typically, a yield of ~60 % is obtained at this step which means approximately 15.000 particles are matched. To improve the number of the matched particles an additional algorithm, called the Neighbour Tracking Reconstruction, is used to approximate a search location for particle images that were not matched. That helped to improv the yield to nearly 85 % (i.e. ~25.000 matched particles). The next step of the process consisted of tracking the matched particles, using a robust matching algorithm, and around ~12.000 individual randomly spaced velocity vectors could be obtained from each instantaneous velocity volume. These were interpolated into nearly ~25.000 vectors with a spatial resolution of 1 mm into the three directions when a minimum number of 2 random vectors per node of 4×4×4 mm^3 with an overlap of 50 % was considered.

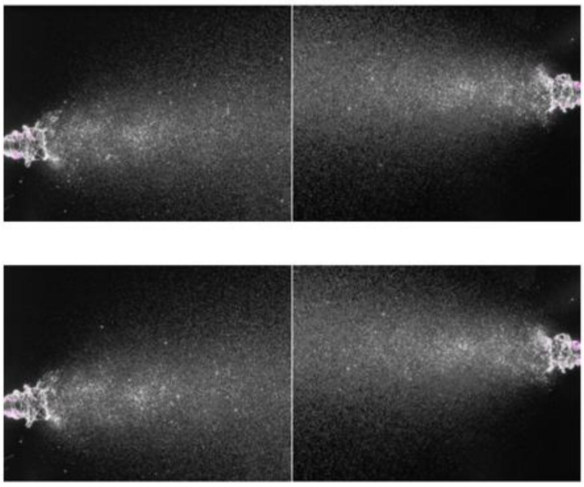

Figure 4. Raw image as seen by cameras

Results

As was mentioned before V3V-Flex© is based on PTV, so the system tracks the particles reconstructed in time t_0 and t_{0+c}. In each experiment more than 30 000 particles were recognized and the system was able to reconstruct more than 15 000 velocity vectors.

The axial velocity was varied from a few meters per second to more than 20 m/s. The spray cone angle can be derived from the particle positions, Figure 6 and 11, or can be obtained by processing the raw images in Figure 5 and 9.

Simplex PSA $P_{in} = 3.5\,Bar$

Simplex PSA $P_{in} = 4.5\,Bar$

Figure 5. Raw images as seen by a single camera

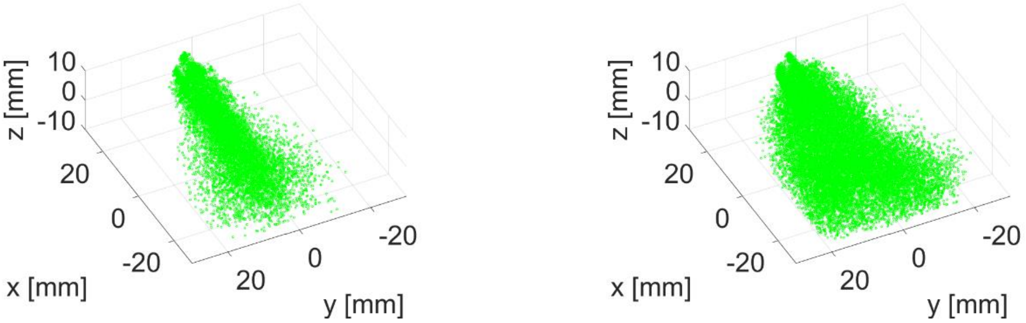

Simplex PSA $P_{in} = 3.5\,Bar$ Simplex PSA $P_{in} = 4.5\,Bar$

Figure 6. Particle position

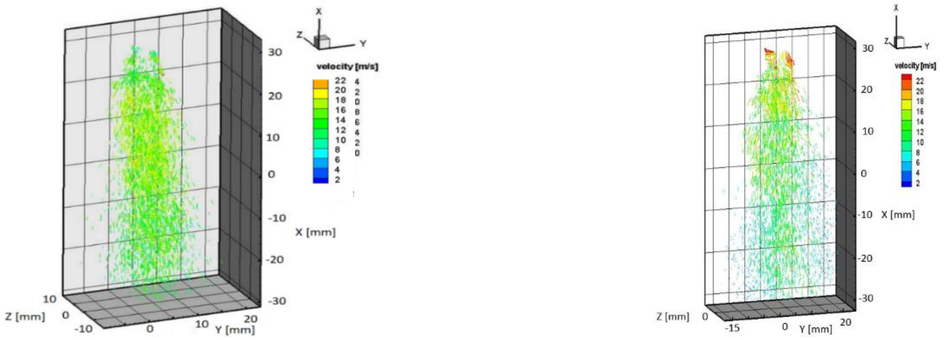

Simplex PSA $P_{in} = 3.5\,Bar$ Simplex PSA $P_{in} = 4.5\,Bar$

Figure 7. Velocity vector field

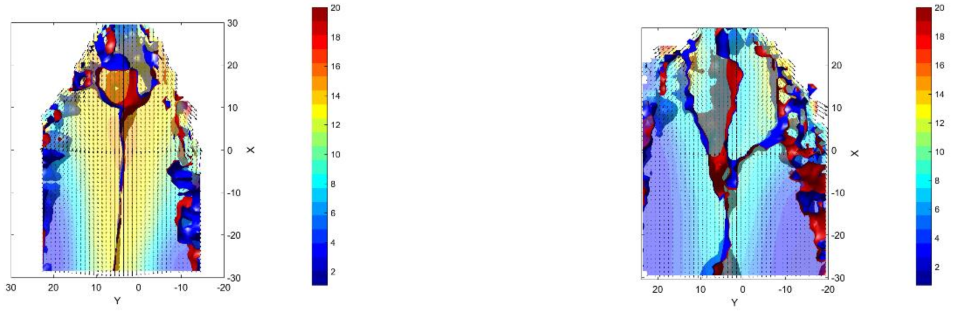

Simplex PSA $P_{in} = 3.5\,Bar$ Simplex PSA $P_{in} = 4.5\,Bar$

Figure 8. Average velocity magnitude and Z vorticity (i.e. isosurfaces)

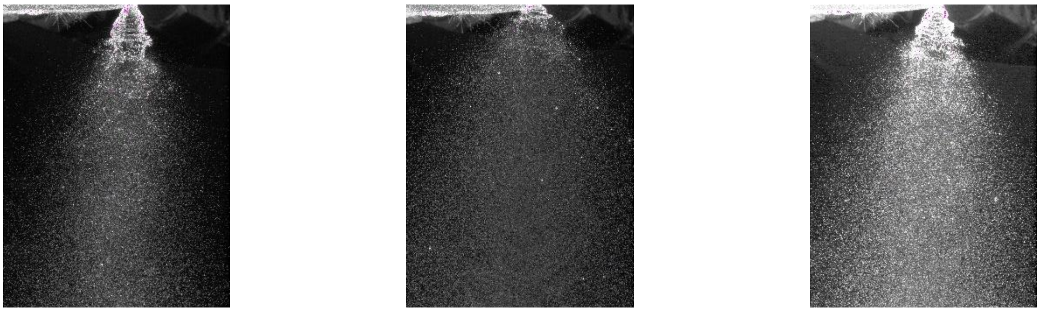

SL nozzle $P_{in} = 3.5\,bar$, SL = closed SL nozzle $P_{in} = 4.5\,bar$, SL = closed SL nozzle $P_{in} = 4.5\,bar$, SL = open

Figure9. Raw images of a spray as seen by the single camera

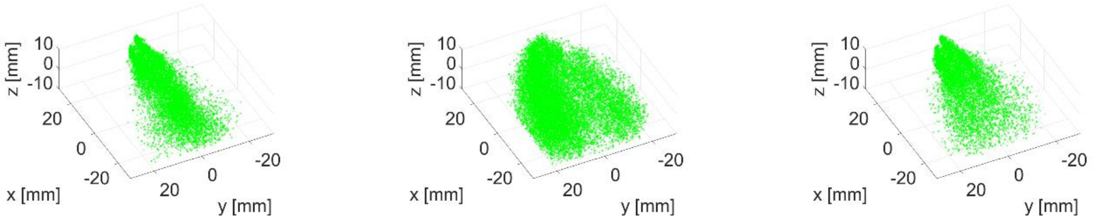

SL nozzle $P_{in} = 3.5\ bar$, SL = closed SL nozzle $P_{in} = 4.5\ bar$, SL = open SL nozzle $P_{in} = 4.5\ bar$, SL = closed

Figure10. Particle position

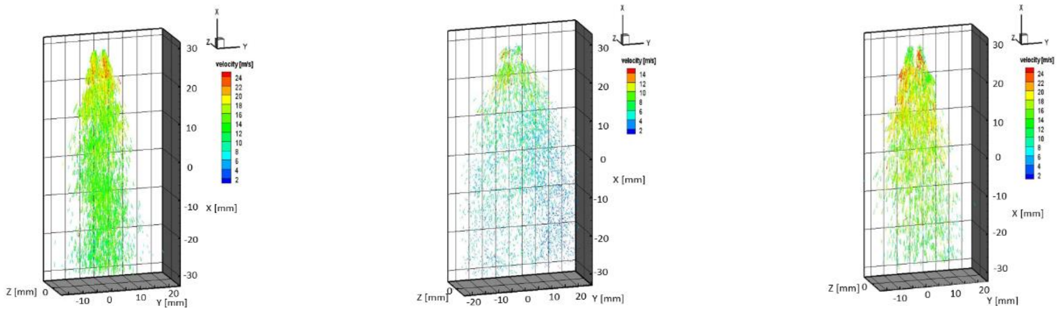

SL nozzle $P_{in} = 3.5\ bar$, SL = closed SL nozzle $P_{in} = 4.5\ bar$, SL = open SL nozzle $P_{in} = 4.5\ bar$, SL = closed

Figure11. Velocity vector field

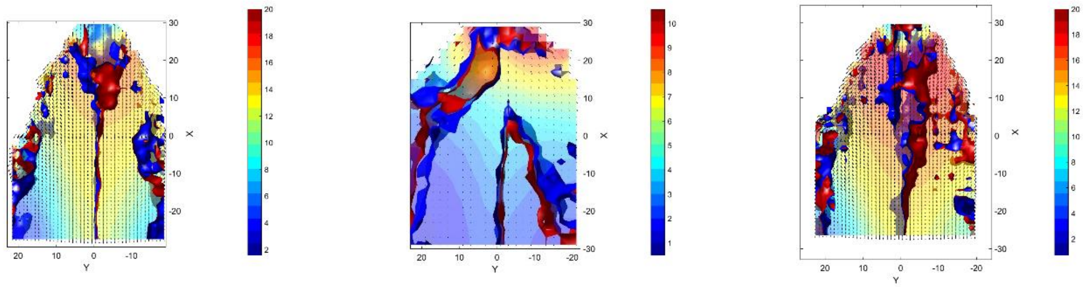

SL nozzle $P_{in} = 3.5\ bar$, SL = closed SL nozzle $P_{in} = 4.5\ bar$, SL = open SL nozzle $P_{in} = 4.5\ bar$, SL = closed

Figure12. Average velocity and Z vorticity (i.e. isosurfaces)

Figures 5 to 8 compare the Simplex pressure swirl atomizer operating with different inlet pressures. Figure 6 shows the particle position of the simplex pressure atomizer at different inlet pressures. The wider spray cone angle can be observed at an inlet pressure of 4.5 bar. This change of spray cone angle can also be derived from the raw images in Figure 5. From this figure some denser areas in the spray can be recognized. Velocity vector fields are shown in Figure 7. At the inlet pressure of 4.5 bar, higher velocities of droplets in the spray are readilly observed. It is caused by more pressure energy being available for conversion into kinetic energy. Figure 7 also shows how droplets lose their momentum in the streamwise direction from the discharge orifice. This velocity loss is caused by drag of surrounding medium acting on a droplet surface. In the primary breakup region the velocity ranges from 18 to 22 m/s, in “lower” section of spray velocities are in the range from 4 to 10 m/s. In Figure 8 the average velocity computed from all captured images are shown.

Figures 9 to 12 show the differences between the spill-line nozzles behaviour at different pressures and different spill-line valve adjustment. Figures 9 and 10 show the raw images and particle position respectively, where variations in a spray cone angle with pressure and the SL adjustment can be observed. The difference in spray cone angle between the opened and closed SL is approximately 24 degrees. The difference between the SL nozzle for $\mathrm{P_{in}} = 3.5\ \mathrm{bar}$ (SL = closed) and SL nozzle $\mathrm{P_{in}} = 4.5\ \mathrm{bar}$ (SL = open) is approximately 12 degrees. The SL adjustment also affects the droplet velocity field, Figure 11. The velocity drop between the regimes is caused by a portion of the fluid flowing through the spill-line instead of the discharge orifice, but the spill-line opening has a favourable effect on atomization quality.

Conclusion

This paper has discussed the investigation of two types of pressure swirl atomizers by means of a volumetric the PIV technique, V3V- Flex©, TSI Inc. The difference between the PSA design and the influence of different test conditions, i.e. inlet pressure and SL valve adjustment were readily observed. Changes in droplet velocities and spray cone angles were quantified under the different test conditions. It is apparent, from Figure 11, how different pressure conditions and SL adjustment influences the spray created by the spill-return pressure swirl atomizer. The Spill-line pressure swirl atomizer with a closed SL valve works similar to a simplex atomizer and also the spray behaviour is very similar, Figure 7 and 11. The measurement volume size set for the experiment was 45 ×60 ×20 mm. This size of measurement volume was restricted only by the size of spray droplets used as the flow tracers and by the laser power. Results obtained are found to be in agreement with the PSAs theory and the suitability of V3V-Flex© for spray flows investigation is proved in this study. PSAs are used mainly in combustion areas, where droplets sizes and its spatial distribution are very important characteristics of a spray. For droplet size information it is good to combine V3V- Flex© with another measurement technique such PDA, which allows point wise measurement

Acknowledgement

The authors acknowledge the financial support from the project No. 18-15839S funded by the Czech Science Foundation and the project “Computer Simulations for Effective Low-Emission Energy” funded as project No. CZ.02.1.01/0.0/0.0/16_026/0008392 by Operational Programme Research, Development and Education, Priority axis 1: Strengthening capacity for high-quality research

.

References

[1] Jedelský, J., Malý, M., Corral, N., Wigley, G., Janáčková, L., Jícha, M., 2018, International Journal of Heat and Mass Transfer, 121, pp. 788-804.

[2] Lízal, F., Jedelský, J., Morgan, K., Bauer, K., Llop, J., Cossio, U., Kassinos, S., Verbanck, S., Ruiz-Cabello, J., Santos, J., Koch, E., Schnabel, Ch., 2018, European Journal of Pharmaceutical Sciences, 113, pp. 95-131.

[3] Cejpek, O., Malý, M., Feb. 20.-22. 2019, Topical Problems of Fluid Mechanics 2019.

[4] Lefebvre, A.H., 1989, “Atomization and sprays.”

[5] Malý M., Sapík M., Cejpek O., Wigley G., Katolický J., Jedelsky J., 2019, Experimental Thermal and Fluid Science, 106, pp. 159-170.

[6] Boomsma, A., Troolin, D., Lai, W., Sep. 14.-16. 2015, 11TH INTERNATIONAL SYMPOSIUM ON PARTICLE IMAGE VELOCIMETRY – PIV15.